

UNITED STATES DEPARTMENT OF THE INTERIOR
GEOLOGICAL SURVEY

Liquefaction Potential of the Yukon Prodelta, Bering Sea

by

Edward Clukey, David A. Cacchione, and C. Hans Nelson

This report is preliminary
and has not been edited or
reviewed for conformity with
Geological Survey Standards
and nomenclature.

ABSTRACT

The Yukon **prodelta** is exposed to large storm waves propagating northward from the southern Bering Sea. Shallow water depths of the prodelta enhance the transfer of energy from the surface waves to the bottom. As the bottom deposits are cyclically loaded by large storm waves, potential decrease in their resistance to shear could ultimately cause liquefaction. A preliminary assessment of the engineering properties of Yukon sandy silt suggests that the prodelta deposits may be susceptible to wave-induced liquefaction during severe storm events. In addition, erosion and resuspension of sediment in the prodelta may be intensified because of the liquefaction process.

INTRODUCTION

The stability of granular sea-floor deposits can be upset by liquefaction of the deposits under cyclic loading and their behavior as a viscous fluid. This liquefaction or **fluidization** of bottom sediment may pose severe problems to the integrity of offshore installations. The bearing capacity of the sea floor beneath offshore structures (Lee and Focht, 1975; Rahman et al., 1977) may be seriously impaired if the upper few meters of deposits liquefy and mass flows result. Erosion and sediment scouring caused by current-induced bottom shear stresses are other processes significantly related to liquefaction vulnerability. The net effect may be the erosion of foundation-bearing sediment beneath platforms sited on the bottom. The extent of the damage potential would depend on the **areal** distribution of the liquefiable material and recognition of the liquefaction potential in design considerations.

The liquefaction of sea-floor sediment results from repeated loading during either earthquakes or high-intensity storm **waves**, when pore-water pressures reduce the shearing resistance of the material. In this report we

consider the potential of Yukon prodelta deposits (Fig. 1) to liquefy under large-amplitude surface water waves. Although Norton Basin does possess several active faults that could pose a moderate seismic risk, the **liquefaction** potential under wave loading is considered particularly destabilizing on the basis of sediment-type (borderline sand-silt) in the prodelta (Fig. 2) and exposure of the prodelta to large storm waves. **Typical** late-fall storms in Bering **Sea** generate large-amplitude low-frequency waves that propagate into Norton Sound from the southern Bering Sea. Water depths (Fig. 1) throughout Norton Sound are also sufficiently shallow (<20 m), that most ,wave-generated surface energy is imparted to the bottom deposits. Under these conditions, bottom deposits may liquefy during storms. To investigate this possibility, we have made a preliminary assessment of the liquefaction potential of Yukon prodelta deposits.

This study was in part based on samples from, and bottom-pressure measurements in, the Yukon prodelta (Fig. 1). At present, however, no direct cyclic strength data have been gathered on undisturbed samples from the area, and thus our conclusions should be considered tentative. This assessment of **the** liquefaction potential was supplemented by results obtained by other investigators on similar sediment. The dissipation of pore-water pressures for a typical and an extreme storm event was modeled by an isoparametric **one-**dimensional finite-element method (**FEM**) of analysis. Although our **results** are not site specific, they do represent the general sea-floor conditions throughout the prodelta area and provide insights for more detailed studies aimed at defining the degree of liquefaction susceptibility on a regional basis, using techniques recently devised for onshore deposits (**Youd** and Perkins, 1978).

DATA COLLECTION

Data for this investigation were collected aboard the research vessel Sea Sounder during 1976, 1977, and 1978. Bottom pressure measured at 2.2 m above the sea floor and current measurements taken at 1 m above the sea floor were recorded with a multi-instrumented bottom tripod, GEOPROBE (Cacchione and Drake, 1979), used to investigate sediment transport on continental shelves. The GEOPROBE (Fig. 3) collected 80 days of bottom data during July-September 1977 at a water depth of 19 m approximately 50 km south of Nome, Alaska (Fig. 1). During that time, data were collected on one moderate storm that generated 3-m surface waves with approximately 10- to 12-s periods (Fig. 4).

Core samples were taken with a variety of coring devices including shallow grab samplers as well as 2- and 5-m vibracoring samplers (Fig. 1). Only rarely did core stratigraphy appear to be disturbed by coring.

The cores were **subsampled** at sea immediately after collection, typically at the core surface and at 0.5-m intervals thereafter, and above and below distinct stratigraphic changes. Grain-size distributions were determined from **subsamples** using wet-sieve splits made at 2 mm (Sieve 18) and at 0.0625 mm (sieve 230), and the mud fraction was run in a hydrophotometer measuring **silt** and clay grain sizes less than 0.0625 mm (Clukey and others, 1978).

Bulk densities were determined on a few whole-core sections before opening. Generally, the in-situ density was estimated by taking small plugs of known volume. The densities of samples could also be determined from their water content (assuming 100-percent pore-water saturation). Appropriate corrections were made in all cases for the salinity of the pore water. Minimum and maximum densities were calculated on the basis of mean grain size and sorting characteristics of the deposits, and from results obtained by other investigators on approximately similar types of deposits.

GEOLOGIC AND OCEANOGRAPHIC SETTING

The Yukon prodelta is in the southwest part of Norton Sound in the northern Bering Sea (Fig. 1). During the Pleistocene, tundra-derived peat deposits formed when the entire northern Bering shelf, including Norton Sound, was emergent because of lowered sea levels (Nelson, in press). These peaty deposits generally overlie Pleistocene glacial and alluvial deposits that are underlain by pre-Quaternary bedrock. About 12,000 years **B.P.** Sphanberg Strait (Fig. 1) was flooded during sea-level transgression, and transgressive fine sand and silt began to be deposited there. By 9500 **B.P.** Norton Sound had been inundated by water, and modern Holocene sandy-silty mud began prograding over the Pleistocene freshwater peaty mud (Nelson and **Creager**, 1977). The modern Yukon **subdelta** moved north to its present position about **5000** years **B.P.** or later.

The Yukon River presently carries **60** to 100 million tons of sediment into the Bering Sea each year (**Lisitsyn**, 1966). Currents transport much of the Yukon-derived sediment into the **Chukchi** Sea (Drake and others, 1980). Sediment remaining in Norton Sound is deposited onto a **deltaic** wedge that thickens from **2-** to 10-m depth toward the modern Yukon **subdelta** (Fig. 2) (Nelson and **Creager**, 1977). The southwest margin of the prodelta consists of well-sorted silty sand grading northward to moderately sorted silty sand and eastward to poorly sorted sandy silt and silt (**Dupre** and Thompson, 1978). The Holocene sandy and silty mud of the Yukon River (Fig. 2) covers central and northern Norton Sound with **surficial** deposits as thick as 2 m. **Chirikov** basin, west of Norton Sound is entirely bypassed, and no modern very fine sand and silt are deposited there (Nelson, in press).

Investigation of large-scale current patterns in the northern Bering and **Chukchi** Seas were summarized by Coachman and others (1976). The regional

circulation is relatively simple: Bering shelf water flows northward into the Arctic basin throughout most of the year. This flow is principally driven by sea-level differences across the Bering Strait and is modified by surface-wind stresses generated by large-scale atmospheric-pressure systems. Surface-wind stresses associated with the predominant northerly winds decrease the magnitude of this northward flow and occasionally reverse the surface-current direction. When the flow is northward, topographic constriction approaching the Bering Strait effectively enhances the current speed north of about latitude 64°30' N. Bottom deposits in the approaches to the Bering Strait are predominantly made up of sand that has been molded into a variety of **bedforms** characteristic of progressively stronger bottom currents.

Energetic atmospheric storms normally transit the northern Bering Sea with increasing frequency, commencing in September. Typically, these early storms have low-pressure centers that pass north of Nome, Alaska. These storm tracks are favorable for the formation of large surface waves by sustained strong southwesterly winds blowing across a relatively unimpeded fetch that terminates along the outer northern margin of Norton Sound (Fig. 1). Such conditions have historically caused intense storm surges and extensive wave erosion of the Nome coastline (Sallenger and Dingier, 1978).

Monthly averages of sea state and winds compiled by the Arctic Environmental Information and Data Center (1977) indicate that over the last 35 years, in the northwestern Bering Sea (the area contained within latitude 60°N and the coastline to longitude 175° W). the maximum observed wave heights have been 7 m in September and 8 m in October. The statistical recurrence interval for extreme waves of 24-m height in the deeper southernmost part of the study area is only 5 yr; the maximum significant wave height for this same recurrence period is 13.5 m (Arctic Environment Information and Data Center,

1977, p. 438). At Nome, Alaska, the recurrence period for sustained windspeeds of 50 knots is 5 yr. We note that during the period November 11-13, 1974, a storm surge estimated to be a **once-in-30-yr** occurrence severely damaged the Nome area; during this storm an estimated water rise of 7.6 m caused extensive flooding over the entire north margin of Norton Sound (Sallenger and Dingier, 1978). Normal tidal range for that period was 1.2 m.

These data indicate the extreme importance of wind-driven and wave events in the study area. Estimates of bottom erosion and sediment transport must include measurement and evaluation of not only normal fair-weather turbulent shear stresses but also excessive stresses induced by high waves.

LIQUEFACTION OF A SEDIMENTARY DEPOSIT

Temporary or permanent loss in the strength of ocean deposits generally occurs in loose **fine-grained** sand to coarse silty sediment (Lee and Fitton, 1969). In extreme cases, this loss in strength can cause liquefaction of the deposits. Liquefaction is controlled by the buildup of excess pore-water pressures, that is, above hydrostatic, as the deposits are subjected to cyclically induced shear stresses. As the material responds to these shear stresses, the particles tend to compact. If the permeability of the deposits is insufficient to allow for instantaneous reorientation of the particles, excess pore-water pressures develop. As these pressures increase with successive cycles, the deposits weaken and become less resistant to the imposed load. The shear resistance is then associated with a critical level of repeated loading (Sangrey and others, 1978). As pore-water pressures dissipate over time, the particles tend to move closer together, and the deposits become more stable. If the rate of pore-water-pressure dissipation is sufficiently rapid relative to the rate of pore-water-pressure generation,

the deposits will remain stable under the prevailing load. If, however, the applied load is sufficient to overcome dissipation effects, the deposits will tend to fail and may ultimately liquefy.

The permeability of the deposits controls the rate of pore-pressure dissipation. Thus, the more permeable the deposits, the greater will be the critical level of repeated loading required to induce liquefaction. In an earthquake-related situation, in which the frequency of loading is relatively high, pore-water-dissipation effects are generally negligible. The loading frequencies for storm waves, however, can be an order of magnitude less than those associated with earthquake frequencies, so dissipation of pore-water pressures over time must be considered.

Deposits that are sufficiently dense before loading do not generate long-term positive excess pore-water pressures. The soil particles in these deposits after finite displacements tend to dilate when sheared and thereby generate a negative pore-water pressure that temporarily increases the strength of the deposit. The relative density D_r , numerically expresses the relation of the onsite density to the maximum and minimum densities of the deposits; that is,

$$D_r = \frac{\gamma_{\max} (\gamma - \gamma_{\min})}{(\gamma_{\max} - \gamma_{\min})} \quad (1)$$

where: γ = the in-situ dry unit weight

($\gamma = \rho g$, where ρ = density and

g = acceleration due to gravity)

γ_{\max} = the maximum dry unit weight of sediment

and γ_{\min} = the minimum dry unit weight of sediment

This relative density commonly is used as an index for the density state of granular material. Deposits with greater relative densities tend to be less

susceptible to liquefaction and therefore require higher critical levels of repeated loading in order to liquefy. The liquefaction potential then depends on the integrated effects of:

- (1) the density state of the deposits,
- (2) the level of loading imposed by storm waves,
- and
- (3) pore-water-dissipation effects.

A fourth parameter, the relation between the effective confining stress and the density state of the deposits, is also important in evaluating the liquefaction potential. Unfortunately, more detailed laboratory data are necessary before its importance can be assessed. In the absence of these data, in the present study we consider the deposits to be normally consolidated, and so the density state, level of loading, and dissipation effects will govern the response.

LIQUEFACTION ASSESSMENT

To evaluate the liquefaction potential from wave loading, we can effectively apply techniques used in earthquake engineering with some minor modifications (Nataraja and Singh, 1979). Once the level of imposed stresses has initially been determined, the number of cycles required to liquefy the sediment calculated under undrained conditions, at a given relative density, can be calculated (Seed and Rahman, 1978). The effects of drainage on bed response can then be modeled by an FEM analysis (Seed and Rahman, 1978). This model includes the dissipation of pore-water pressure after the passage of each wave. The total pore-pressure buildup as a function of the overburden pressure is then continually monitored throughout the duration of the storm or until 100-percent pore-water-pressure response is achieved. Although 100-percent pore-water-pressure response is not necessarily sufficient for

liquefaction, it does represent a condition whereby at least a temporary loss in strength occurs as a result of excess pore-water pressures.

WAVE-INDUCED STRESSES

Several techniques are presently available to determine both the pore-water-pressure response and the cyclically imposed shear and normal stresses in the deposits (Fig. 5). Moshagen and Tørum (1975) used the heat-conduction equation, together with the assumptions that the pore-water is incompressible and that the porous bed is unreformable, to predict the transitory wave-induced pore-water-pressure response; these responses are infiltration pore-water pressures, not those associated with shear stresses. This approach, however, does not predict the induced stresses in the deposits. Other investigators (Prevost and others, 1975), concerned with bed deformation and the resulting stresses, assumed the bed to be elastic and not to interact with the pore-water; the conclusions reached from this approach are those derived from classical solid mechanics. More recently, Yamamoto (1978) and Madsen (1978) have used a three-dimensional consolidation model for the bed to predict the wave-induced pore-water-pressure and effective-stress changes in the bed during a single wave cycle. The results of their work indicate that the bed response is strongly affected by the permeability and stiffness of the sediment as well as by the thickness of the bed.

None of these solutions, however, considers the response of the bed under repeated loading. Pore-water pressures would increase under application of cyclic shear stresses. This increase in pore-water pressure varies as a function of the number of applied loads, that is, waves, and reduces the normal effective stresses acting on the bed. This increase in pore-water pressure also depends on the drainage characteristics, frequency of loading, and duration of loading. Seed and Rahman (1977) considered the cyclic-loading

effects of storm-generated waves and proposed an FEM solution to model the pore-water-pressure dissipation effects throughout a storm. In their solution the wave-induced stresses were calculated by considering the total stress state in the bed and applying an appropriate stress function. Their solution is similar to that proposed by Prevost and others (1975). Where the deposits are idealized as a semi-infinite half-space, the expression for the horizontal (1977), is identical to that of Yamamoto (1978) and Madsen (1978); that is,

$$\tau_h = 2\pi\Delta p \left(\frac{z}{L}\right) \exp\left(\frac{2}{L} z\right), \quad (2)$$

where: p = the bottom wave-induced pressure,
 L = the wavelength,
and z = the depth in the sediment.

The geometry is illustrated in Figure 5. If we subtract the pore-water pressures determined by Moshagen and Tørum (1975) from the total stresses, the effective principal stresses are also identical to those determined by Yamamoto (1978) and Madsen (1978).

The horizontal shear stress can then be normalized with respect to the overburden stress σ'_{v_0} , that is,

$$\frac{u'}{\sigma'_{v_0}} = \gamma_b z \quad (3)$$

where: γ_b = the buoyant unit weight of the sediment.

The resulting expression then gives the maximum shear-stress ratio at a depth z :

$$\frac{\tau_h}{\sigma'_{v_0}} = 2 \frac{\overline{\Delta p}}{\gamma_1 b} \exp \left\{ -\left\{ \frac{2\theta}{1} z \right\} \right\}. \quad (4)$$

Once the maximum shear-stress ratio has been determined, the number of cycles required to cause liquefaction under undrained conditions (for a given relative density) can be calculated from an experimental curve similar to that shown in Figure 6. Although data from actual tests performed on Yukon prodelta sediment may differ from these results, the curve in Figure 6 can be used to make a preliminary estimate of the response characteristics of sandy marine deposits under cyclic loading. The shear-stress ratios (τ_c / σ'_{v_0}), with depth for 3- and 6-m surface waves are shown in Figure 7. The 3-m wave was selected to represent the maximum storm conditions recorded by the GEOPROBE, whereas the 6-m wave would have a 1-percent occurrence frequency for the months of September and October (Arctic Environmental Information and Data Center, 1977).

DENSITY STATE

The relative density of the sediment must be determined to correlate the number of cycles required to cause liquefaction at the imposed-stress level (Fig. 6). Higher relative densities would transpose the curve in Figure 6 upward, whereas lower relative densities would transpose it downward. Typical maximum and minimum density values can be estimated from the grain sizes and sorting characteristics of the deposits. The grain-size analyses of several grab samples are summarized in Table 1. The average-uniformity coefficient c_u for this sand (2.2) indicates a well-sorted material. On the basis of data presented by Johnston (1973) for a similar sand, the respective minimum and maximum densities for Yukon prodelta material were estimated at between 1280-

1320 kg/m³ and 1600-1630 kg/m³. These values were increased slightly to take into account the average percent fines in the samples tested (Townsend, 1973). The final minimum and maximum densities were then estimated to be 1370 and 1760 kg/m³, respectively. These values were somewhat corroborated in tests by other investigators (Lee and Focht, 1975) on marine sediment from the North Sea with similar grain-size characteristics ($d_{50} = 0.11$ mm, $C_u = 2.0$). Their results show minimum and maximum densities of 1340 and 1740 kg/m³, respectively, in good agreement with the values in this study.

Thus, relative density of typical Yukon prodelta sediment can be calculated on the basis of estimated minimum and maximum densities, and the in-situ densities determined from water-content or bulk-density estimates (Table 2). Although the relative densities obtained using the above methods rely on limited data and are initial estimates, they do suggest that the relative density of deposits throughout the study area varies considerably and is not restricted to a unique value or range of values. Thus, pockets or lenses of loose material could conceivably exist throughout the prodelta that would be susceptible to pore-water-pressure generation and possible liquefaction. Despite the variations in the data, a relative density of 54 percent is considered an approximate upper estimate for the sediment within the prodelta. Several of the higher relative densities listed in Table 2 are attributable to dense layers of different material within the stratigraphic section, or to compaction due to vibracoring action.

LIQUEFACTION SUSCEPTIBILITY

We can assess the liquefaction susceptibility for undrained conditions by correlating the number of cycles necessary to cause liquefaction with the shear-stress ratio (τ / σ'_{v_0}), as shown in Figure 6. The 3-m storm-wave height would appear to require an extremely large number of cycles to cause

liquefaction, and the deposits would be even less susceptible if drainage were allowed to occur throughout the storm. Failure, as defined by Egan and Sangrey (1978), could possibly occur, however, if an effective-stress approach similar to Yamamoto's (1978) and Madsen's (1978) were used and the entire stress state were considered in the analysis. On the basis of our analysis, the likelihood of liquefaction from storm waves of 3-m height appears extremely small.

For the 6-m storm wave height, however, full pore-water-pressure response could occur in the upper several meters of sediment within a relatively small number of cycles under undrained conditions in the bed. If drainage were allowed, a greater number of cycles would be necessary to liquefy the deposits; an FEM analysis can then be used to investigate the effects of drainage during the storm. The 6-m storm-wave height was investigated with this technique for a storm duration of one hour. Because the dissipation effects depend on the permeability and compressibility of the deposits, two different permeability-compressibility combinations were used in the analysis. The buildup of pore pressure for each time increment was governed by the equation

$$r_u = \frac{2}{\pi} \arcsin(x^{1/2\theta} z) \quad (5)$$

where: r_u = the ratio of excess pore-water pressure to initial vertical effective stress,

x = the ratio of the applied cycle (n) to the number of cycles (n_1) required to cause liquefaction,

and θ = an empirical shape constant for the pore-water-pressure curve (1.2 in this analysis).

The results of the analysis indicate (Fig. 8) that even with **pore-water-** pressure dissipation taken into consideration, the deposits will liquefy to a depth of 3 to 3.5 m. The permeability of the material significantly influences the time required for liquefaction to occur. For a coefficient of permeability of $5 \times 10^{-5} \text{ m/s}$, which would correspond to a **medium-** to **coarse-** **grained** sand like that encountered in Chirikov Basin, the sediment would not liquefy. The coefficients of permeability, derived from laboratory consolidation test results (1.5×10^{-6} to $1.5 \times 10^{-7} \text{ ms}$), that represent a range of values typical for Yukon prodelta sandy silt show that liquefaction is possible. In this case pore-water pressure dissipation effects do not preclude full pore-water pressure response and possible liquefaction.

GEOLOGICAL IMPLICATIONS; HAZARD POTENTIAL

The present analysis suggests that modern Yukon prodelta sediment could at least temporarily liquefy to significant depths **during** severe storms. The widespread distribution of **thick** storm-sand layers **within** 50 km of the modern prodelta shoreline (Nelson, 1977) suggests that liquefaction and mass movement processes may be important mechanisms in the movement of major sheets of sand offshore. These sand layers range from 1 cm thick in central Norton Sound to over 20 cm thick within 30 km of the delta (Nelson, 1977). The more massive sand layers close to the delta may in part result from mass movement of liquefied material under major storm-wave and surge conditions. **Bottom-** friction velocities from tidally dominant bottom currents are insufficient to transport massive quantities of material. Drake and others (1980) suggest (from **GEOPROBE** data) that the very fine sand constituting about 50 percent of the sediment on the outer part of the Yukon prodelta is mostly transported during a few late summer and fall storms each year. The mean transport velocities for the September 1977 storm that generated 3-m-high waves, as

recorded by the **GEOPROBE**, were well in excess of those required to initiate transport of sediment (**Cacchione** and Drake, 1980). The effects of this transport mechanism during more severe storm events would be magnified if the bed were partially softened by liquefaction and the zone of material influenced by the mean transport velocity were several meters thick. Integration of the liquefaction susceptibility with the critical mean transport velocity in future sediment-transport models could provide useful insights into the rate and amount of sediment transport in this area.

Severe erosional effects can be observed in the delta area in the form of large scour depressions (Larsen and others, 1979). These depressions, which range as large as 250 m in diameter and 1 m in depth, are triggered by local topographic disruptions in prodelta areas where strong currents shear against steeper offshore topography. The potential for liquefaction in this area may greatly enhance the formation of these scour depressions. Weakening of the deposits by increased pore-water pressures, along with mixing of the deposits with water by storm-wave action, could lead to erosion and transport of sediment from scour depressions.

Liquefaction to a depth of 2.5 to 3 m and consequent movement of massive storm-sand sheets could cause severe hazards to sea-floor structures; this is particularly true if the protective sedimentary cover were removed from buried pipelines, or the sea floor around foundations were undermined. The undermining of a foundation can be partly predicted by more extensive and detailed site investigation, whereas pipeline construction must rely on a more regional data base and interpretation. Techniques similar to those presented herein would be useful in the selection of possible pipeline routes leading to onshore terminal facilities.

Preliminary strength tests on several samples from the study area (Olsen and others, 1979) suggest that some of the Yukon prodelta sediment may be significantly **overconsolidated**. This overconsolidation is due to the removal of past higher stresses from the deposits or the effects of a constant wave stress over a prolonged period. The **overconsolidation** leads to increased shear resistance in the deposits. For deposits with the same relative density, those that are overconsolidated would be less prone to liquefy (Seed, 1977) than those that are normally consolidated. Additional tests are **required**, however, for a more comprehensive assessment of such overconsolidation effects on the liquefaction potential.

SUMMARY

The vulnerability of Yukon prodelta sandy silt to wave-induced liquefaction has been evaluated using engineering analysis and data on **storm-**wave and sediment characteristics. The combination of sediment type, exposure to large storm systems, shallow water depths, and at least some fairly loose layers of material suggests that the prodelta may be susceptible to the generation of excess pore-water pressures and to consequent loss in strength and ultimate liquefaction. Geologic evidence of potential liquefaction effects includes the presence of prograded storm sand sheets and fairly broad scour depressions throughout the prodelta area.

We adapted methods currently practiced in earthquake engineering to our analysis, which considers two simplified storm systems. The principal difference between the **earthquake-** and storm-wave-based analyses is a longer duration for the storm event and consequently greater dissipation of **pore-**water pressures. A 3-m surface wave height was found to be insufficient to liquefy the deposits, even when the effects of pore-water-pressure dissipation were neglected. However, a storm event with 6-m wave heights theoretically

would generate 100-percent pore-water-pressure response and liquefaction in the sediment to a depth of approximately 3.5 m in one hour. Recent preliminary strength tests, however, indicate significant overconsolidation of the same Yukon deposits that may decrease the liquefaction danger, although **the** significant reduction in strength within the upper several meters of sediment may remain as a hazard to construction in the study area. Liquefaction, coupled with the shallow gas-charged deposits that are widespread in this area, (Nelson and others, 1979), may further complicate foundation engineering. Additional testing, however, is clearly needed before any final assessment **of** the extent of hazard potential can be properly made.

ACKNOWLEDGMENTS

The authors thank David Drake for his assistance with the GEOPROBE analysis and Devin Thor for his compilation of the Yukon sediment isopach map. This study was supported in part by the U.S. Geological Survey and the Bureau of Land Management through interagency agreement with the National Oceanic and Atmospheric Administration, under which a **multiyear** program responding to the needs of petroleum development of the Alaskan Continental Shelf is managed by the Outer Continental Shelf Environmental Assessment Program (OCSEAP) office.

REFERENCES

- Arctic Environmental Information and Data Center, 1977: Climatic Atlas of the outer continental shelf waters and coastal regions of Alaska, v. 2, Bering Sea, Anchorage, University of Alaska, 443 p.
- Beckman, W.J., 1970, Engineering considerations in the design of ocean outfall: Journal **WPCF**, v. 42, no. 10, p. 1805-1831.
- Brown, R.J., 1971, How deep should an offshore line be buried for protection: Oil and Gas Journal, v. 69, p. 151-155.
- Cacchione, D.A., and Drake, D.E.**, 1979, A new instrument to investigate sediment dynamics on continental shelves: Marine Geology, v. 30, p. 299-312.
- Cacchione, D.A., and Drake, D.E.**, 1980, Storm-generated sediment transport on the Bering continental shelf, Alaska: Journal of Geophysical Research, in press.
- Clukey, E.C., Nelson, H.C., and Newby, J.E.**, **Geotechnical** properties of **northern** Bering Sea Sediment: U.S. Geological Survey Open-File Report 78-408, 29 p.
- Coachman, L.K., Aagaard, **K.**, and Tripp, R.B., 1976, Regional Physical Oceanography: Seattle, University of Washington Press, 186 p.
- Drake, D.E., **Cacchione, D.A., Muench, R.D., and Nelson, C.H.**, 1980, Sediment transport in Norton Sound: Marine Geology, in press.
- Dupré, W.R., and Thompson, R.**, 1979, A model for **deltaic** sedimentation in an **ice** dominated environment, Offshore Technology Conference, Houston, Texas: Proceedings, Paper 3434.
- Egan, J.A., and Sangrey, D.A.**, 1978, Critical state model for cyclic load pore pressure: Proceedings of ASCE **Geotechnical** Engineering Division Specialty Conference, Pasadena, California, Earthquake Engineering and Soil Dynamics, p. 410-424.
- Holmes, M.L., and Thor, D.R., 1980, Distribution of gas-charged sediment in Norton Basin, northern Bering Sea, in Nio, S.D., Van den Berg, J.H., and **Siegenthaler, C.**, eds.: International Association of Sedimentologists, International meeting on Holocene **marine** sedimentation in the North Sea Basin, in press.
- Johnson, J.L., and Holmes, **M.L.**, 1978, Surface and subsurface faulting in Norton Sound and **Chirikov** Basin, Alaska, in Environmental Assessment of the Alaskan continental shelf, Annual **Report** of Principal Investigators, Environmental Research Laboratory, Boulder, Colorado, v. 12, p. 203-227.
- Johnston, M.M.**, 1973, Laboratory studies of maximum-minimum densities of **cohesionless** soils, in The evolution of relative density and its role in **geotechnical projects involving cohesionless** soils, **Selig** and Ladd, eds.: ASTM STP 523, p.133-140.

- Kvenvolden, K.A., Nelson, C.H., Thor, D.R., Larsen, M.C., Redden, G.D., Rapp, J.V., and Des Marias, D.J., 1979, Biogenic and thermogenic gas in gas-charged sediment of Norton Sound, Alaska: Offshore Technology Conference, Houston, Texas: Proceedings, Paper 3412, p. 479-483.**
- Larsen, M.C., Nelson, C.H., and Thor, D.R., **1979, Geologic** implications and potential hazards of scour depressions on Bering shelf, Alaska: *Environmental Geology*, **v. 3**, p. 39-47.
- Lee, **K.L., and Fiton, J.A., 1969, Factors affecting the cyclic loading strength of soil: ASTM STP 450, p. 77-95.**
- Lee, K.L., and **Focht, J.A., 1975, Liquefaction potential of Edofisk Tank in North Sea, Journal of the Geotechnical Engineering Division, ASCE, v. 100, no. GT1, p. 1-18.**
- Lisitsyn, A.P., 1966, Recent sedimentation in the Bering Sea, Moscow, Akad., Nauk, SSSR; English Trans., 1969, Israel Program of Scientific Translation (Springfield, Virginia, U.S. Dept. of Commerce Federal Science Technical Information), 614 p.**
- Madsen, O.S., 1978, Wave induced pore pressures and effective stresses in a porous bed: *Geotechnique*, v. 28, no. 4, p. 377-393.
- Moshagen, H., and Trum, A., 1975, Wave induced pressures in permeable seabeds, Journal of Waterways, Harbors and Coastal Engineering, ASCE, v. 101, no. WW1, p. 49-58.**
- Nataraja, M.S., and Singh, H., 1979, A simplified procedure for ocean-wave-induced liquefaction potential: Proceedings of Civil Engineering in the Oceans, Special Conference IV by ASCE Technical Council on Ocean Engineering, v. 2, p. 949-963.**
- Nelson, **C.H., 1977, Storm surge effects, in: Environmental assessment of the Alaskan continental shelf: Annual Report of Principal Investigators, U.S. Department of Commerce, Environmental Research Laboratory, Boulder, Colorado, v.18, p. 120-129.**
- Nelson, C.H., **1980, Holocene transgression in deltaic and non-deltaic areas of the Bering epicontinental shelf, in Proceedings of the International Meeting on Holocene Marine Sedimentation in the North Sea Basin, International Association of Sedimentologists, Nio, S.D., Schuttenhelm, R.T., and Weering, T.C.E., eds., 30 p., in press.**
- Nelson, C.H., and **Creager, J.S., 1977, Displacement of Yukon sediment from Bering Sea to Chukchi Sea during Holocene time, Geology: v* 5, p. 141-146.**
- Nelson. C.H., Thor, D.R., **Sandstrom, M.W., and Kvenvolden, K.A., 1979, Modern biogenic gas-generated craters (sea-floor "pockmarks") on the Bering shelf, Alaska: Geological Society of America Bulletin v. 90, p. 1144-1152.**

- Olsen, H.E., **Clukey**, E.C., and Nelson, C.H., 1979, **Geotechnical** characteristics of bottom sediments in the northern Bering Sea, in Proceedings of the International Meeting on Holocene Marine Sedimentation in the North Sea Basin, International Association of **Sedimentologists**, **Nio**, S.D., **Schuttenhelm**, RoT., and **Weering**, T.C.E., eds., p. 91-92.
- Prevost, J.H., Eide, O., and Andersen, K., 1975, Wave induced pressures in permeable seabeds: Journal of Waterways, Harbors and Coastal Engineering, ASCE, v. 101, no. ww4, p. 464-465.
- Sallenger**, A.H., Jr., and Dingier, J.E., 1978, Coastal processes and **morphology** of the Bering Sea coast of Alaska, Final Report of Research Unit **431** in Outer continental shelf environmental assessment Program, Juneau, Alaska, National Oceanographic and Atmospheric Administration, U.S. Department of Commerce, 66 p.
- Sangrey**, D.A., Castro, G., **Poulos**, S.J., and France, J.W., 1978, **Cyclic** loading of sands, **silts**, and clays: **ProceeCalifornia**, of ASCE **Geotechnical Engineering Division** Conference, Pasadena, Earthquake Engineering and Soil Dynamics, p. 836-851.
- Seed, H.B., 1979, Soil liquefaction and cyclic motility evaluation for **level** ground during earthquakes: Journal of **Geotechnical Engineering Division**, ASCE, v. 105, no. **GT2**, p. 201-255.
- Seed, H.B., and **Rahman**, M.S., 1978, Analysis for wave-induced pore pressure relation to ocean floor stability of **cohesionless** soils: **Marine Geotechnology**, v. 3, no. 2, p. 123-150.
- Townsend, F.C., 1973, Comparisons of vibrated density and standard compaction tests on sands with varying amounts of fines, **in** The evaluation of relative **density** and **its role in geotechnical projects** involving **cohesionless** soils, **Selig and Ladd**, eds., ASTM STP 523, p. 348-363.
- Yamamoto**, T., **1978**, Sea bed instability from waves, Offshore Technology Conference, Houston, Texas: Proceedings, Paper 3263, p. 1819-1824.
- Youd**, T.L., and Perkins, D.M., 1978, Mapping liquefaction induced ground failure potential: Journal of the **Geotechnical Division**, ASCE, v. 104, no. **GT4**, p. 433-446.

TABLE 1

Table I.--Results of grain-size analyses of sediment
samples from the Yukon prodelta

Box core	Core Depth (cm)	Sand (%)	Silt (%)	Clay (%)	d_{60} (mm)	d_{10} (mm)	$c_u = d_{60}/d_{10}$ ¹
164	4	96.9	2.6	0.4	0.187	0.101	1.83
166	11	92.6	6.3	1.1	0.135	0.072	1.86
162	12	86.0	12.3	1.7	0.108	0.042	2.58
168	11	90.6	7.9	1.5	0.109	0.062	1.76
157	4	77.2	22.1	0.7	0.101	0.035	2.89

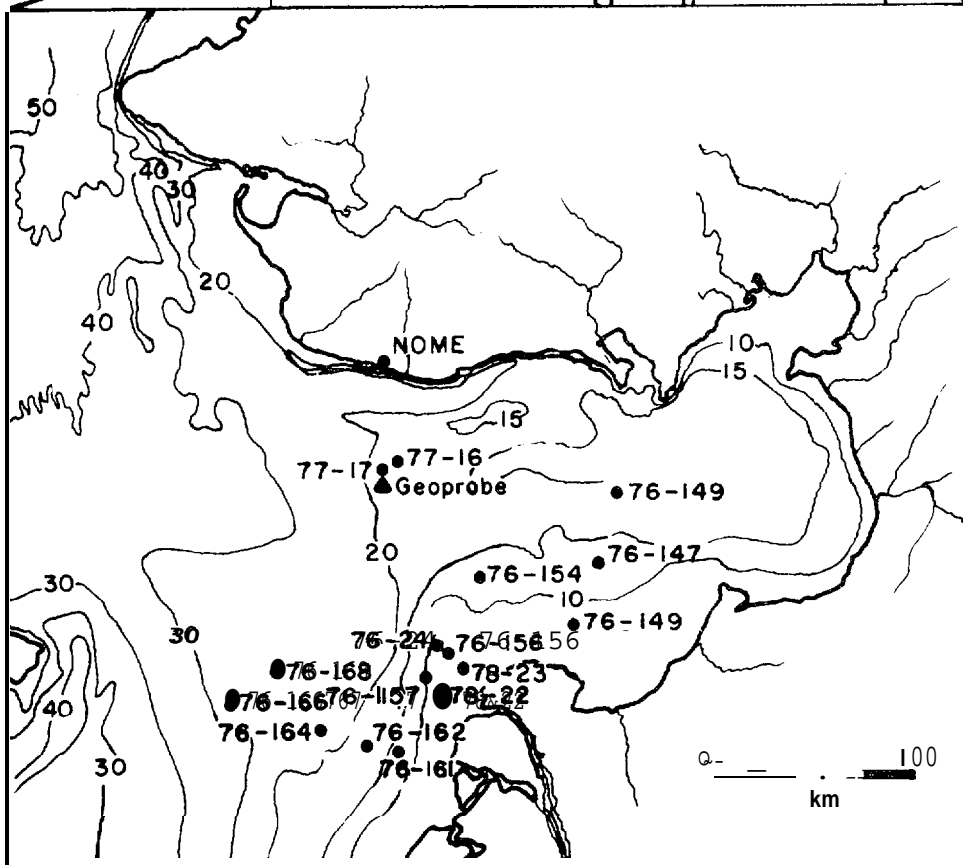
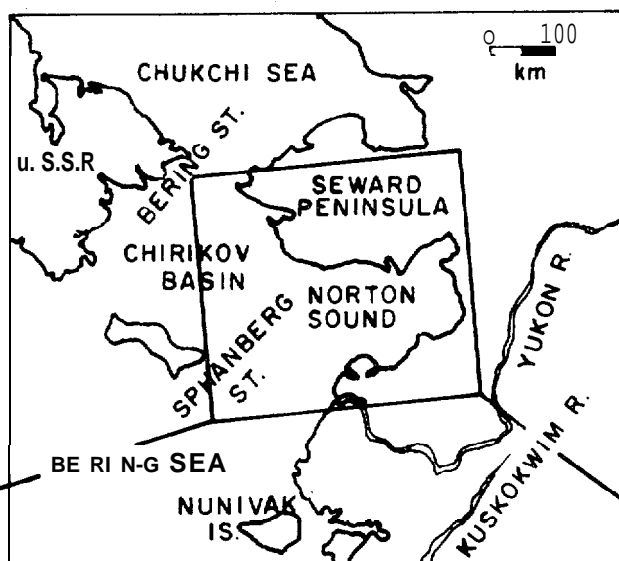
¹Average = 2.18

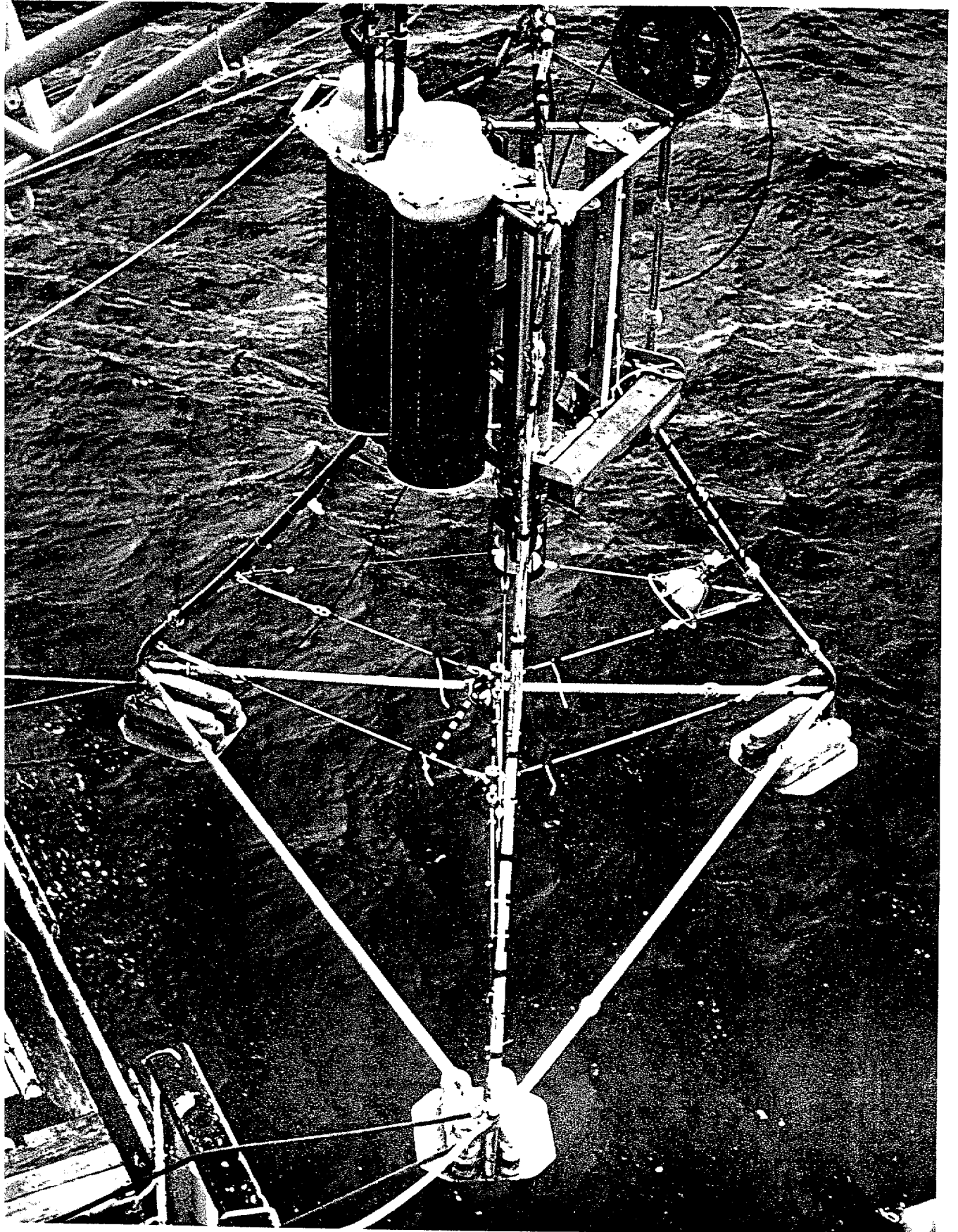
Table 2.--Density data on samples from Norton Sound

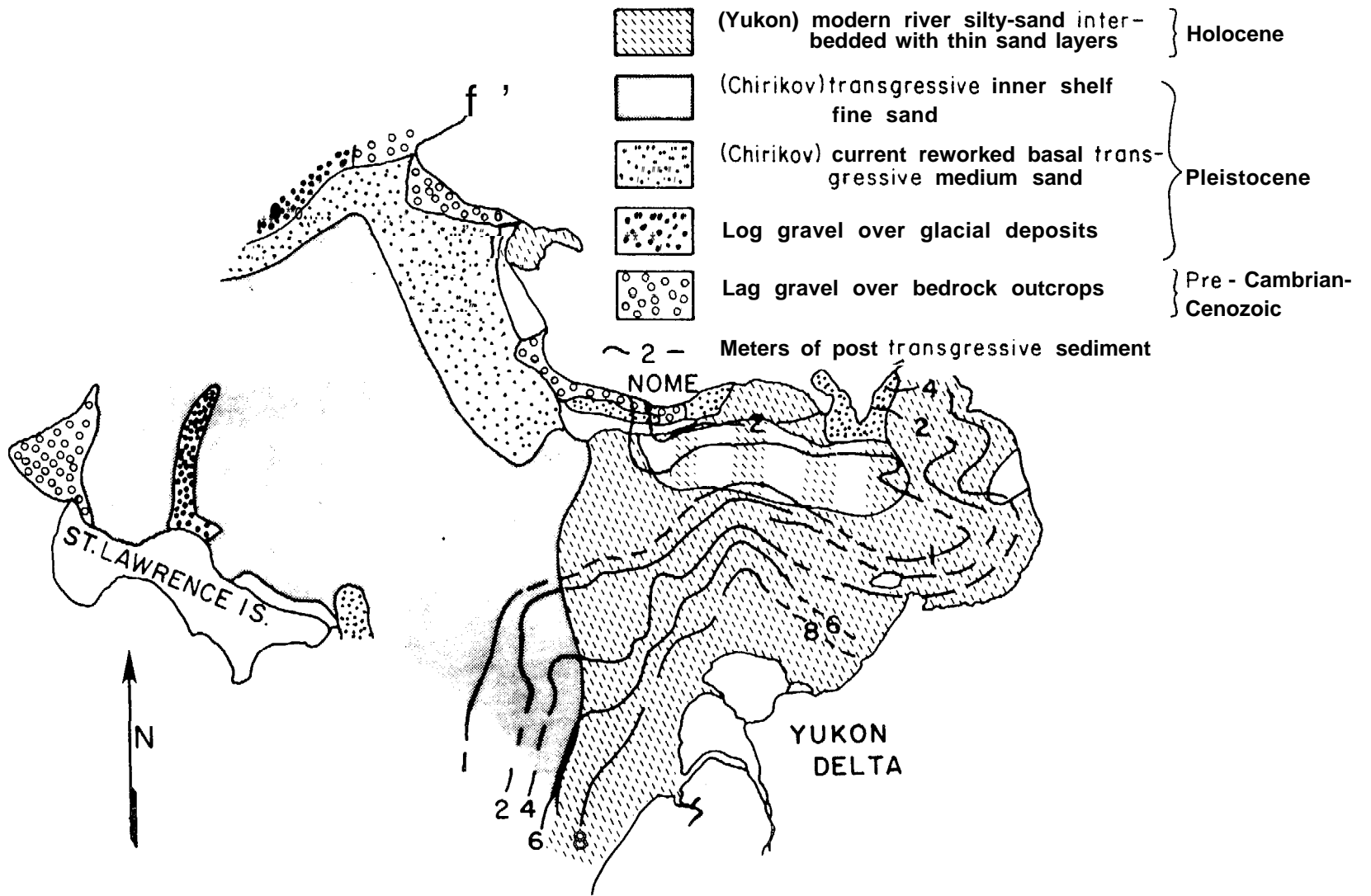
Location	Depth (cm)	Water content (%) corrected	Dry unit weight γ (lbs/ft)	Dry density (Kg/m)	Relative density D_r
L47	2-6	30.9	96	1.54	51
L149	Surface	106.1	45	0.72	*
L54	4-5	43.0	72	1.15	*
	13-14	56.1	70	1.12	*
	10-18	46.6	77	1.23	*
	26-29	45.0	80	1.28	*
L56	33-35	81.7	55	0.88	*
L61	2-12	51.8	73	1.17	*
Core					
L7	6-8	37.6	87	1.39	9
	23-25	37.8	85	1.36	*
	40-42	31.6	94	1.51	42
	54-56	34.5	90	1.44	26
	72-74	32.3	93	1.49	39
	90-92	31.7	94	1.51	43
	123-125	73.3	59	0.95	*
	134-136	26.5	102	1.63	*
L17	0-2	35.9	89	1.43	18
	8-10	49.1	75	1.20	*
	13-15	39.5	84	1.35	*
	18-20	38.0	86	1.38	*
	24-26	29.1	99	1.59	58
	19-21	42.7	81	1.30	*
Core					
L16	10-12	30.6	96	1.54	49
	29-31	33.3	92	1.47	33
	39-41	26.9	101	1.62	69
	49-51	29.2	98	1.57	57
	64-66	28.3	99	1.59	62
	74-76	27.2	100	1.60	68
	84-86	26.6	101	1.62	71
	109-111	22.0	109	1.75	98
	119-121	19.3	114	1.83	100
	129-131	28.7	98	1.57	59
	139-141	24.0	106	1.70	87
L27A	0-3	44.7	77	1.23	.
	5-7	37.6	84	1.35	*
	15-17	35.4	87	1.39	22
	18-20	41.1	82	1.31	

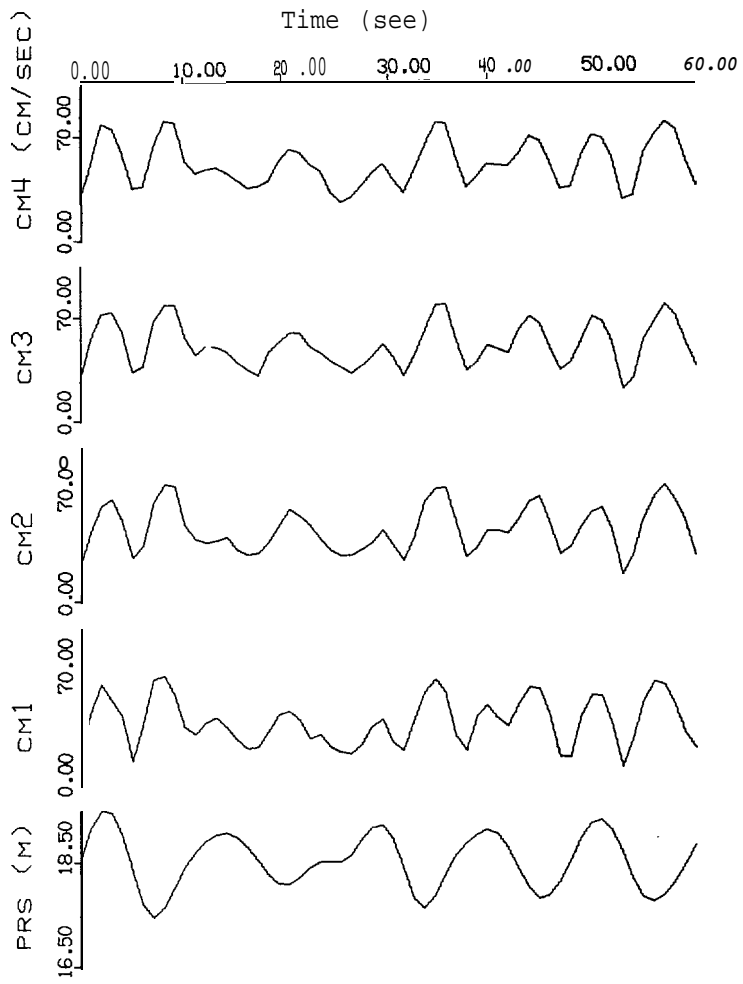
Figures

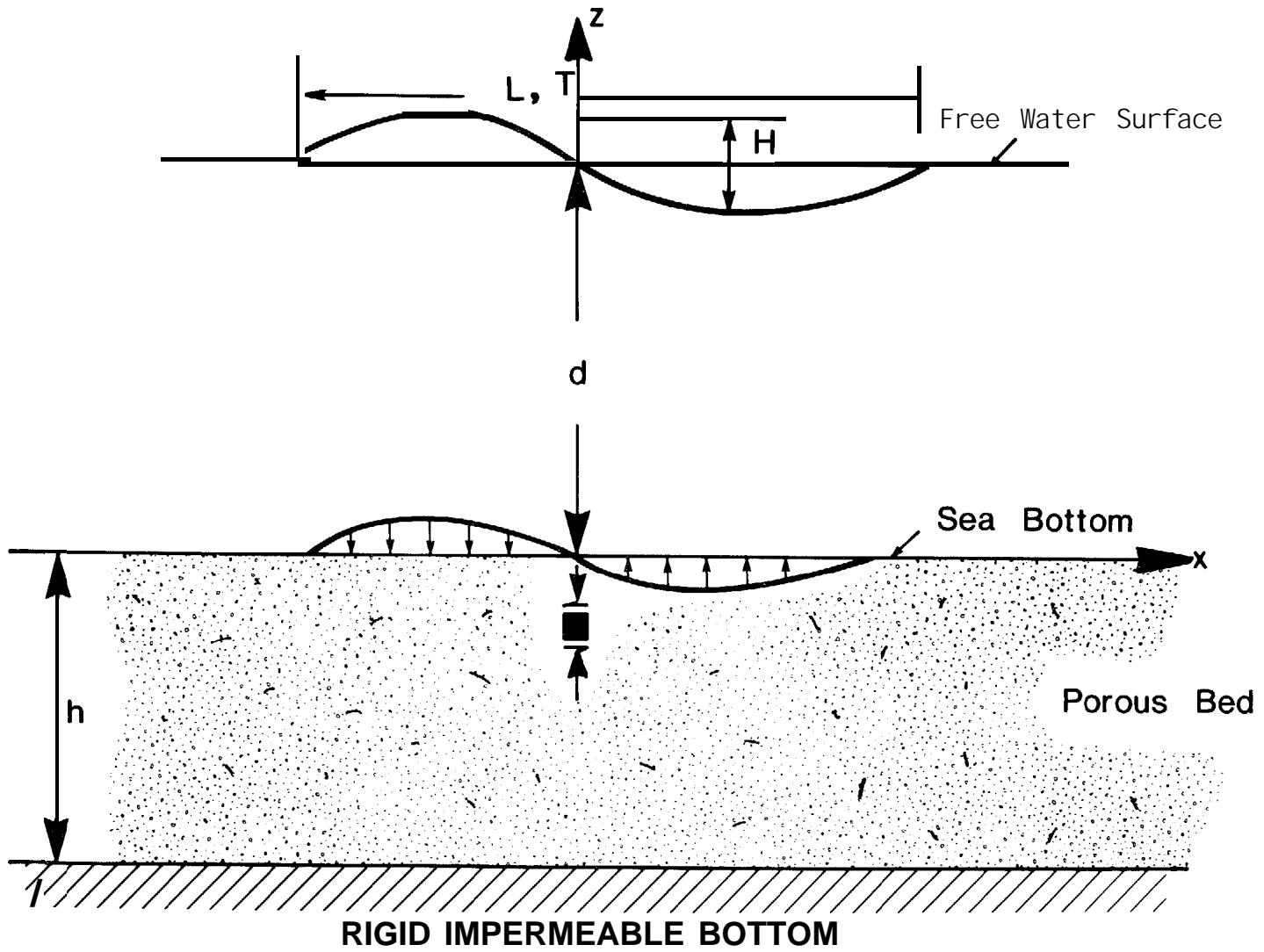
- Figure 1.** Station locations for core samples taken during 1976, 1977, and 1978 field seasons; site of GEOPROBE deployment during July-September 1977. The Yukon prodelta extends out to 90 km into North basin; isopach contours in Figure 2.
- Figure 2.** Surficial sediment distribution in Norton Sound (modified after Nelson, 1980) and isopach thickness of Holocene-Yukon derived sediment (modified after Thor, in prep.).
- Figure 3.** GEOPROBE tripod during launch into Norton Sound, July 1977. Horizontal distance between attachment points of footpads is 3.2 m; overall height is about 3.5 m. Flotation package in upper part of photograph rests on plastic (PVC) buckets containing recovery line. Current sensors are visible within center of tripod. Undersea strobe attached to leg at right; pressure cases contain electronic systems and sensor packages (see Cacchione and Drake, 1979).
- Figure 4.** Current-meter and pressure data taken with GEOPROBE during storm on Sept. 14, 1977, in Norton Sound, Alaska. Data were taken every second for 60 s. Current speeds (computed from north-south and east-west components) at 0.2, 0.5, 0.7, and 1 m above sea floor are designated by CM1, CM2, CM3, and CM4, respectively. Pressure (PRS) is measured at 2 m above sea floor and expressed in equivalent meters of water. Averages have not been removed from data.
- Figure 5.** Simplified wave profile used in liquefaction-potential analysis. Bottom-pressure wave data were obtained from linearized wave theory. Bottom pressures induce horizontal shear stresses that cause a pore-water-pressure response and reduced strength.
- Figure 6.** Normalized cyclic horizontal shear-stress ratio (τ_h / σ'_{v0}) vs number of cycles required for initial liquefaction (undrained conditions) for deposits with a relative density of 54 percent (Seed, 1977).
- Figure 7.** Wave-induced shear stress ratio (τ_h / σ'_v) vs depth (Z) for 3- and 6-m-surface wave heights during storm events.
- Figure 8.** Results of preliminary analysis of wave-induced liquefaction potential of Holocene Yukon sandy silt near Yukon prodelta: H, wave height; T, wave period; D_r , relative density; K, coefficient of permeability; u / σ'_v ratio of wave-induced excess pore-water pressure to initial effective overburden stress.
-

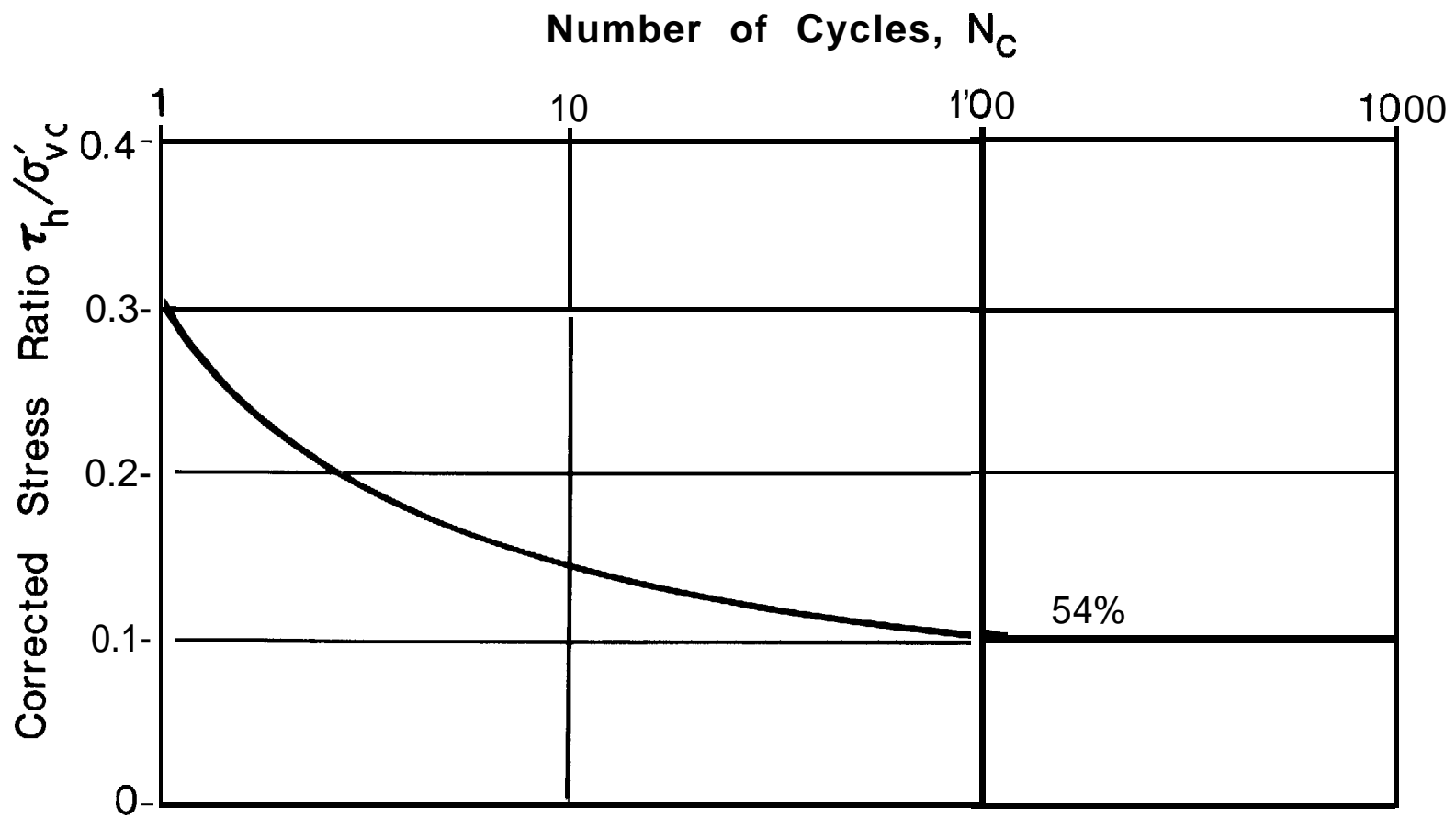




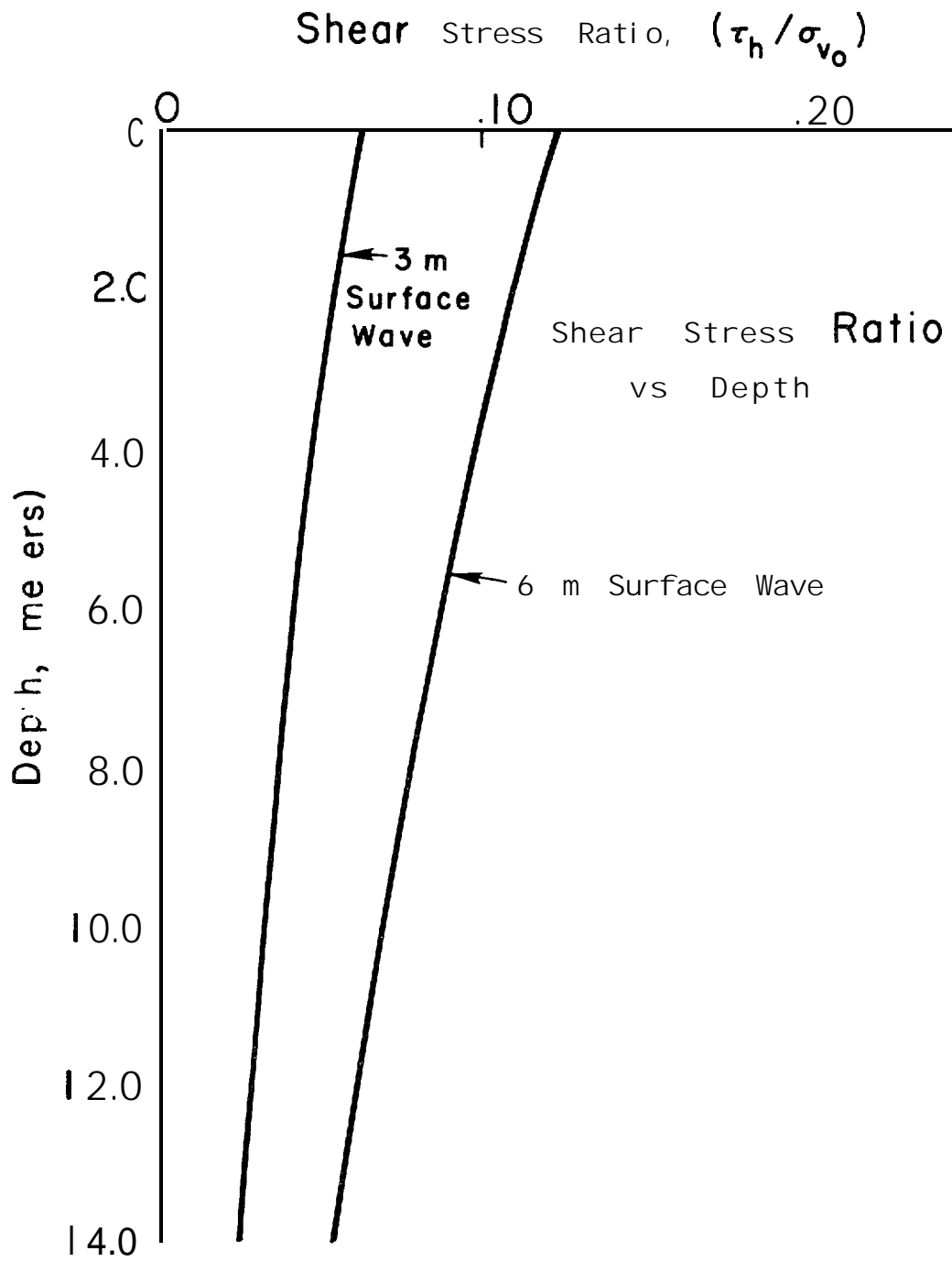


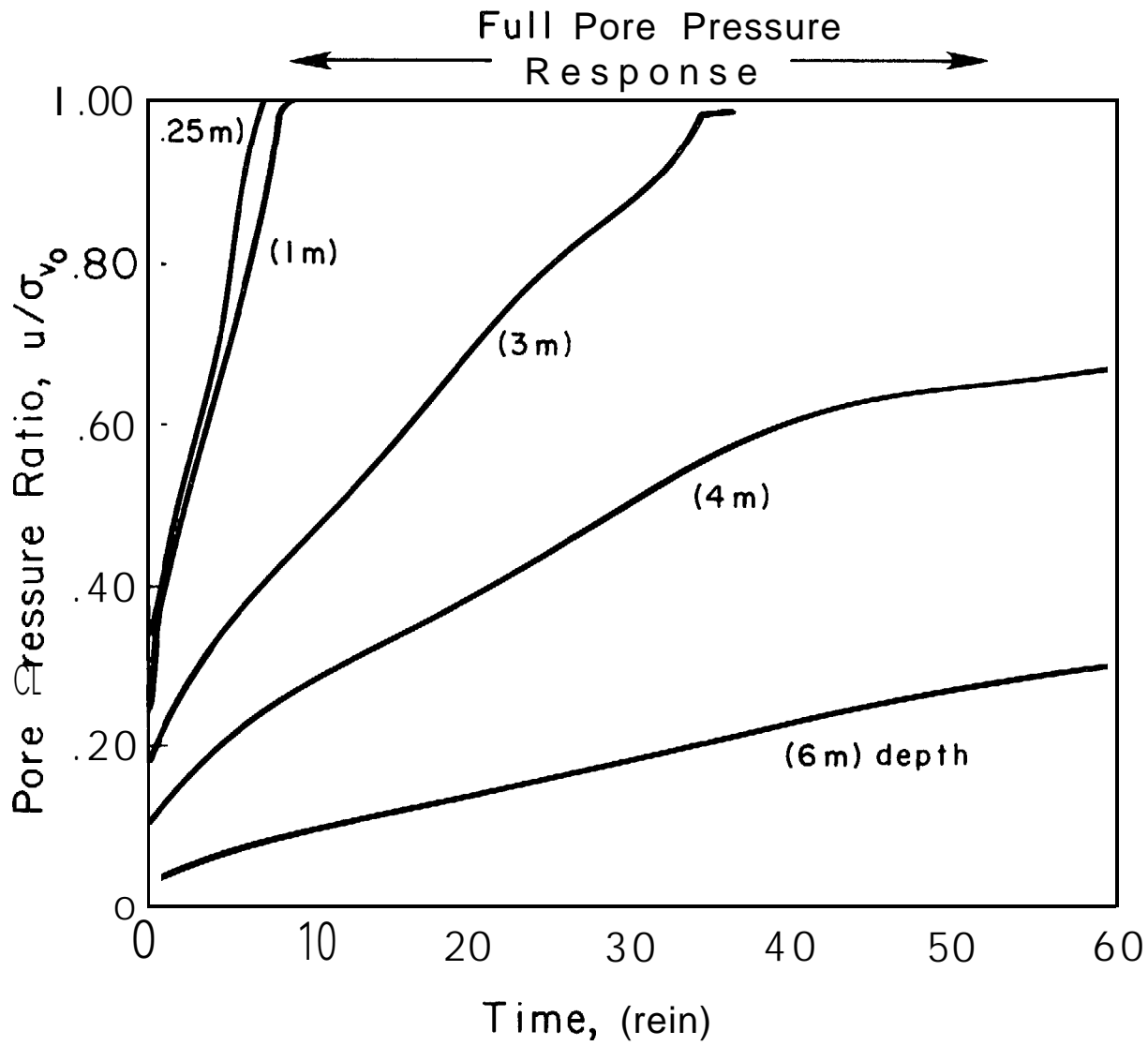






CORRECTED τ_h/σ'_{v0} VS. N_C FOR INITIAL LIQUEFACTION





Wave
Liquefaction Analysis

Norton Sound

H = 6 m, T = 10 s

$D_r = 54\%$

$k = 1.50 \times 10^{-6}$ m/sec